Chiroptical Applications Enabled by Integrated Photonic Waveguides

(Student Paper)

J. Enrique Vázquez-Lozano, Alejandro Martínez
Nanophotonics Technology Center, Universitat Politècnica de València, Camino de Vera s/n, 46022 Valencia, Spain
e-mail: juavazlo@ntc.upv.es

ABSTRACT

Chiral spectroscopy is a routine technique for identifying the chirality of matter through optical means. So far, all the approaches to analyze the chirality of chemical analytes or artificial nanostructures consider arrangements in which the input light propagates through free space. A similar conception for chiral sensing and spectroscopy may also be applicable in integrated photonic platforms. This would bring about numerous practical benefits such as miniaturization, massive parallel detection, low-cost and large-volume production, repeatability, portability, or integration with electronics, among others. Here we show that all-dielectric integrated photonic waveguides can support chiral modes under proper combination of fundamental eigenmodes. Specifically, we analyze numerically two different scenarios in which such waveguides could be used for chiroptical applications: waveguides as near-field probes for excitation and read-out of chiral light-matter interaction (in-gap configuration), and evanescent-induced chiral interaction (on-top configuration). For simplicity, a metallic nanohelix modeled as a PEC is regarded as a chiral probe, though it would be extensible to other geometries and materials more relevant. Our results may open up new perspectives towards chiroptical applications, such as sensing or spectroscopy, in silicon-based integrated photonic platforms compatible with standard CMOS technology.

Keywords: optical chirality, circular dichroism, chiral sensing, chiroptical spectroscopy, integrated photonics.

1 INTRODUCTION

Chirality is the geometrical property by which an object cannot be superimposed on its mirror image. At the molecular level it plays a key role from a practical point of view, since enantiomers, i.e., pairs of stereoisomers having opposite handedness or chirality, may have well different pharmacological effects [1]. Besides in the geometrical aspects of molecules or structures, chirality is also present in some elementary particles such as photons, leading up to the optical chirality, which, has been recognized as a fundamental property of light characterizing the local handedness of the electromagnetic (EM) field in free-space [2]. Recently, it has been put forward a general and closed expression for the optical chirality, extending the original definition so as to include field propagation through dispersive and even lossy media [3]:

$$C = \frac{\omega}{4c^2}\mathrm{Im}[(\varepsilon(\omega)\mu_{\mathrm{eff}}(\omega) + \varepsilon_{\mathrm{eff}}(\omega)\mu^*(\omega))\,\mathbf{E}\cdot\mathbf{H}^*], \tag{1}$$

where c is the speed of light in free space, $\mathbf{E}$ and $\mathbf{H}$ are, respectively, the electric and magnetic complex field amplitudes, with the asterisk denoting complex conjugation, and ε and μ stand for the material parameters.

Information about the chirality of matter at the micro or even molecular scale can be directly retrieved just by making it interact with chiral light. In this regard, notice that circularly polarized light (CPL) is typically considered as the paradigmatic example of chiral light [2]. There are a number of techniques to discriminate enantiomers, but the most commonly performed is the so-called circular dichroism (CD) spectroscopy, which consists in determining the differential absorption rate of left (L) and right (R) CPL when propagating through a chiral medium [4]. The efficiency of this asymmetric chiroptical response is generally expressed in terms of the dissymmetry factor:

$$g = 2\left[\frac{A^+ - A^-}{A^+ + A^-}\right], \tag{2}$$

where $A^{\pm}$ is the absorption rate of L-CPL (+) and R-CPL (-). This establishes a standard metric to quantify the enantioselectivity and its possible enhancement with respect to CPL. Importantly, in the dipolar approximation, it has been proved that this dissymmetry factor [Eq. (2)] is, in turn, proportional to the optical chirality density [Eq. (1)], thereby providing an enlightening manner to manage the enhanced chiroptical response via an all-optical approach, namely, regardless of the geometric characteristics of the chiral analyte [5].

In recent years there have been many efforts to implement sensing and spectroscopy applications in photonic integrated platforms. In all these cases, light is guided on a circuit through lossless dielectric nanowires, wherein some integrated elements are included to perform the required optical processing. Motivated by this current trend towards full-integrated devices, we explore the existence of (enhanced) optical chirality in integrated dielectric waveguides for its potential application in conventional chiroptical functionalities such as sensing or spectroscopy [6]. While keeping the same working principle, the integrated approach yields many practical advantages, mainly if realized onto silicon-based platforms compatible with standard CMOS technology.

2 CHIRAL RESPONSE IN STRIP WAVEGUIDES: NORMAL INCIDENCE (IN-GAP CONFIGURATION) AND EVANESCENT-INDUCED CHIRAL INTERACTION (ON-TOP CONFIGURATION)

We start by considering a guiding system consisting of a silicon nitride (Si_3N_4) strip waveguide with square cross-section that, for simplicity, is surrounded by vacuum. The fundamental eigenmodes of these structures, typically referred to as transverse electric (TE) and transverse magnetic (TM), yield no chirality. Still, it can be shown that a net optical chirality of opposite signs can arise from the adequate superposition of two orthogonally polarized guided modes [6], thus giving rise to left- and right-handed circularly polarized guided modes (CPGMs), analogously to the conventional case of L- and R-CPL. Building on this analysis, we first show that such waveguides can be used as near-field tips and probes for excitation and read-out of chiral nanostructures in arrangements equivalent to that routinely performed in CD measurements. To this aim, we investigate a chiral metallic scatterer embedded in a narrow gap separating two silicon nitride waveguides with square cross-section ($w = t = 450$ nm). The chiral nanostructure consists of a 4-turns single helix placed in between the waveguides, being centered and orientated along the propagation axis in the z-direction [see Fig. 1(a)]. To understand the chiral behavior of the helix on account of its geometry itself, i.e., dismissing any potential influence of dispersion or absorption effects, the metal is simply modeled as a PEC. Regardless of the number of turns, a full geometrical description of this complex object is determined by the following set of structural parameters: helix radius (R_{helix}), pitch (p), and helix wire radius (r_{helix}), apart from the handedness, given by a relative phase shift between the x and y coordinates. By properly engineering each of these parameters one can gain control over the main spectral features, tuning the resonance position and depth, as well as the optical activity of the metallic chiral structure. In this case, we consider a right-handed helix with geometrical parameters fixed to $p = 50$ nm, $r_{\mathrm{helix}} = 20$ nm, and R_{helix} set as the control parameter, varying from 100 to 114 nm. Notice that this choice is done so that we can keep constant the gap width, in this case to 240 nm.

We excite either L- and R-CPGM in the input waveguide by controlling the relative phase shift between the TE and TM modes. The light exiting the input waveguide will excite the chiral structure in the near-field, here acting as a probe. The output waveguide will collect the light both scattered by the structure and transmitted from waveguide to waveguide, thus enabling the read-out of the chiroptical interaction. To account for the chiral spectral response, we numerically obtain the transmission and mode conversion spectra for L- and R-CPGM [Fig. 1(b)]. From this, it can be seen that, while L-CPGM is nearly transparent to the presence of the helix, R-CPGM exhibit a narrow transmission dip depending on R_{helix}, thereby providing clear evidence of the underlying optical activity brought about when the handedness of the CPGM coincides with that of the chiral structure. These signals directly translate into an asymmetric response on the transmission spectra, whose strength is characterized by the chiral dissymmetry factor [see Fig. 1(c)].

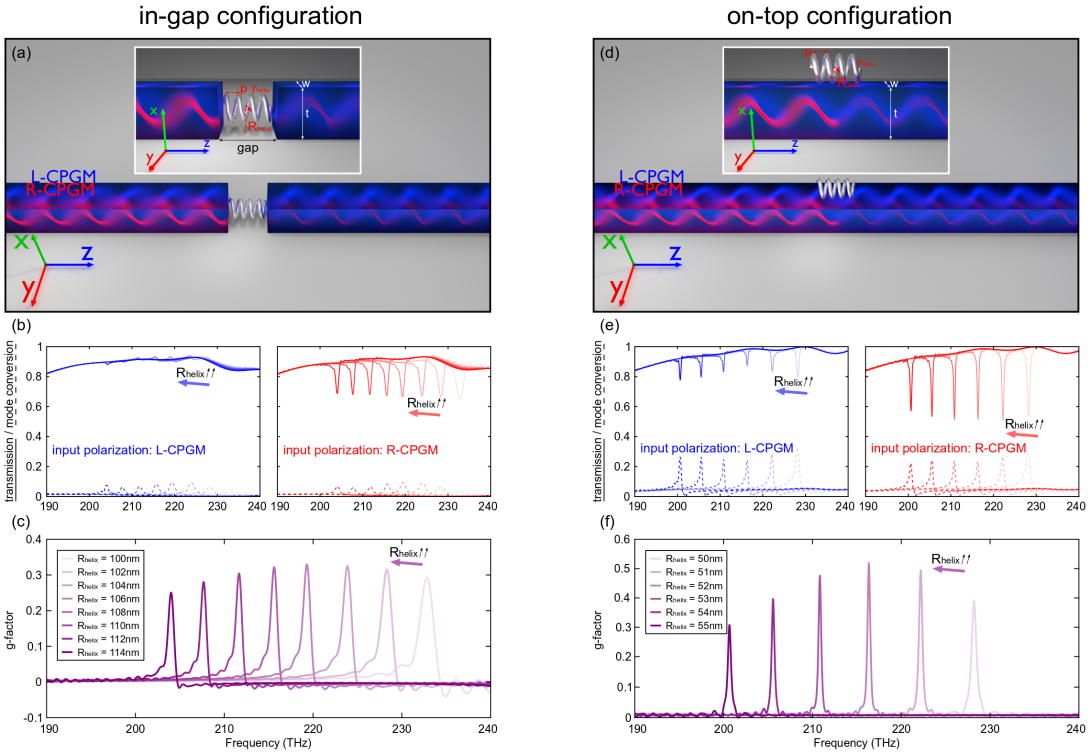

Figure 1. For each configuration: (a,d) Scheme of the arrangement for chiral sensing and spectroscopy enabled by a dielectric strip waveguide; (b,e) numerical simulation of transmission and mode conversion spectra for different values of R_{helix}; (c,f) calculated dissymmetry factor.

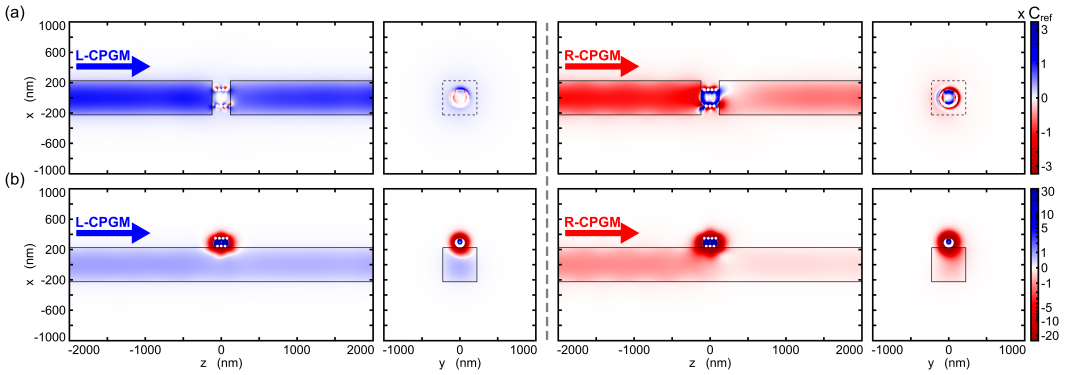

Figure 2. Cross-sectional maps of the optical chirality density for L- and R-CPGM in silicon nitride strip waveguides for (a) the in-gap configuration [Fig. 1(a)] and (b) the on-top configuration [Fig. 1(d)]. In both cases we consider the working frequency $f_{\mathrm{res}} \approx 216$ THz.

A similar analysis holds for the near-field chirality induced by the evanescent field neighboring the silicon nitride square waveguide over which a metallic chiral nanostructure is placed. The scheme of this approach is depicted in Fig. 1(d). Again, maintaining the same geometrical parameters for the nanohelix and modeling it as a PEC, we obtain, via numerical simulations, the spectral behavior of the transmission of L- and R-CPGM for different radii of the helix [Fig. 1(e)]. From these results we can directly calculate the dissymmetry factor g [Fig. 1(f)]. It can be seen that the peaks of g become narrower and higher in comparison with the previous case. This is quite striking since the fields in the evanescent region are much weaker than in the gap spacing two waveguides, wherein they are essentially similar to those in the waveguide core. Yet, this configuration still retain common features with respect to the previous case, in particular, the peak position (or resonance frequency) dependent on the helix radius, and the intermodal conversion between L- and R-CPGM, and vice versa, as a result of the interaction between the CPGMs and the chiral structure.

For a more intuitive description, in Fig. 2 we plot the cross-sectional map of optical chirality density from the corresponding EM field distributions, which are obtained via numerical simulations with the aid of the commercial 3D full-wave solver CST Microwave Studio. This map brings about complementary information to be accounted for. In particular, it provides a clear visualization of the resonant behavior of the nanohelix. Indeed, as shown in Fig. 2, most of the optical chirality density is tightly localized and strongly enhanced in the surroundings of the chiral structure, reaching a value of up to 30 times C_{ref}, i.e., the maximum chirality attainable when the chiral particle is ignored. Remarkably, both the enhancement and the localization are even larger when the input mode possesses the same handedness as the chiral nanohelix, namely, for R-CPGM. This translates into a higher absorption by the particle (or a lower transmission at the output port), thus exhibiting a true chiroptical effect. Regardless of the input mode, the sign of chirality remains uniform in both the outer and the inner region of nanohelix. In this regard, it is worth observing that, inside the helix, the chiral sign is always opposed to that of its handedness. This fact becomes even more evident for the on-top configuration.

3 CONCLUSION AND OUTLOOK

Our results suggest that chiral applications such as sensing and spectroscopy, as well as enantioselectivity, would be feasible using all-dielectric integrated photonic waveguides. Far from providing fully optimized geometries, we only sought to show the viability of this working approach enabled by integrated photonic waveguides. Further considerations should be accounted for a more realistic scenario of chiroptical applications in integrated platforms [6]. In particular, going beyond the ideal PEC model, including dispersion and absorption losses, analyzing the effect of adding a substrate, or investigating the enhancement caused in slotted configurations. At any rate, next steps should be aimed at simplifying both the chiroptical measurement and enhancement schemes.

ACKNOWLEDGMENT

This work was supported by funding from the European Comission Project THOR H2020-EU-829067.

REFERENCES

[1] S. W. Smith, “Chiral toxicology: It’s the same thing...only different,” Toxicol. Sci., vol. 110, pp. 4–30, 2009.

[2] Y. Tang and A. E. Cohen, “Optical chirality and its interaction with matter,” Phys. Rev. Lett., vol. 104, p. 163901, 2010.

[3] J. E. Vázquez-Lozano and A. Martínez, “Optical chirality in dispersive and lossy media,” Phys. Rev. Lett., vol. 121, p. 043901, 2018.

[4] L. D. Barron, Molecular Light Scattering and Optical Activity, Cambridge Univ. Press, Cambridge, 2004.

[5] E. Hendry et al., “Ultrasensitive detection and characterization of biomolecules using superchiral fields,” Nat. Nanotechnol., vol. 5, pp. 783–787, 2010.

[6] J. E. Vázquez-Lozano and A. Martínez, “Towards chiral sensing and spectroscopy enabled by all-dielectric integrated photonic waveguides,” arXiv:1911.11106, 2019.